Chapter 1 – Introduction

Of the multiple modes proposed for quantum computation; one of the first was quantum optics. It is a natural choice for candidacy due the photon's mobility and durability. That is to say that the photon moves quickly while only weakly interacting with its environment. However, despite this, it is because of these strengths that it also lacks. It is difficult to achieve successful photon-photon interactions when the photons are highly mobile and will withstand external interactions. To remedy this, through the combined efforts of Knill, Laflamme, and Milburn; the KLM/linear optical quantum computing (LOQC) was born; and it seeks to make optical quantum computing a reality.

The KLM/LOQC protocol outlines three distinct criteria that must be attained in order to have a successful optical system:

1. Heralded single photon sources with strict mode and bandwidth characteristics

   Heralded indicates the ability to generate entangled photons

2. High-efficiency number resolving single photon detectors

   The chosen detector counts the number of photons incident upon it. Post-measurement, the photon is destroyed, and any state information lost.

3. Construction of complicated optical circuits exhibiting classical and quantum interference effects

We will be addressing the first of three criteria in this thesis. While we have achieved a heralded source in spontaneous parametric down conversion (SPDC). Is it possible for us to do better?

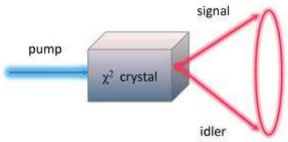

Figure 1.1 General mechanism behind Spontaneous Parametric Down Conversion (Denysbondar, 2012)

Before we continue, let's understand the basic principle behind SPDC. This non-linear optical tool takes in a single photon input which is incident upon a crystal. Upon passing through the crystal, the input photon is split, and outputs entangled photon pairs. The sum of the momenta and energies of the photon pairs total to the initial momentum and energy of the incident photon, which follows in accordance with conservation laws. While this is fascinating, it does not come without its challenges.

SPDC is the most popular entangled photon source, however, is this source deterministic? That is to say, can we produce photons on demand? Determinism will be discussed in detail later on in the thesis but suffice to say that it is not a deterministic source. While it can be guaranteed that an entangled pair is present, if a photon is produced. Producing a photon occurs with an efficiency of 4 outputs for every 10^6 input photons (Matthias, Lenhard, Chunniall, & Becher, 2016). Alternative sources are considered, the most promising of which is the quantum dot, which has the following benefits:

1. On-demand/deterministic generation of single photons or entangled photons
2. Low multi-photon emission probabilities
3. High photon flux
4. Emit indistinguishable photons
5. Numerous tuning mechanisms

But suppose we didn't know any of this? How can we be sure that we are using a quantum system? Outside of entangling capabilities? A method for verifying this is in the detection of Rabi oscillations. In this thesis, we will confirm the quantum nature of the quantum dot by demonstrating the presence of Rabi oscillations. This is done by contrasting a previous model used in experimental fit analysis, for the detection of Rabi oscillations, against an alternative. This alternative will consider environmental effects that may contribute to the damping of the system.

However before this, we must understand the experimental conditions required to replicate this event. An account considering the object measured – the photon, and how the object is produced – the quantum dot. Along with this, we will consider the theoretical background behind Rabi oscillations as well as the analytic method used to generate results – the Linblad Master Equation. Finally in the fourth and fifth chapters there will be a discussion of what was done with detailed findings and resulting conclusions. Coupled with the information from the thesis for PHYS 437 A, I hope that I will be able to demonstrate the viability of this new model. It is my wish that you will learn as much as I have. And so, without further ado, onto chapter two.

Chapter 2 – Experimental and Theoretical Context

Before we can delve into the model, it is important to understand the experimental and theoretical context underlying it. In this section, we will cover the experimental parameters of the object measured – the photon, along with the means of production – the quantum dot. Coupled with this is the theory behind Rabi oscillations – as the phenomenon being modelled and the mechanism behind the model – the Lindblad master equations. These form the backbone for the model being built.

2.1 What is Modelled - Rabi Oscillations

2.1.1 General Intuition

When one thinks of a laser pulse exciting an electron, it is easy to consider it as a one and done phenomenon. However, if we consider the time evolution of this system, we'd find something special. The electron does not experience a single excitation and de-excitation, but a cyclical pattern of this. This phenomenon is called a Rabi oscillation.

Named after Isaac Isidor Rabi, in 1937 Rabi theorized the effect that oscillating electromagnetic fields, that are resonantly tuned to the Zeeman splitting, would have on a spin-½ nucleus. What was found was that the rotating field causes the spin to oscillate, and this became the basis for nuclear

magnetic resonance (NMR) techniques. As a secondary consequence, it served to define Rabi oscillations as well. This is because this process is not unlike oscillations of the electron population when excited by a laser. What's more is that while the oscillation of spin in NMR has a classical description, the repopulation, or revival, in the Rabi oscillations does not (Feranchuk & Leonov, 2008). Suggesting that this is indeed a quantum effect.

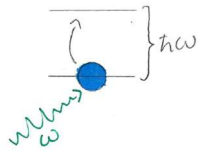

Figure 2.1.1 Two State System Excited by External Light Source

To understand this process further, we turn to the derivation found in Mark Fox's Quantum Optics. Let us consider a simplified model: suppose we consider a simple two-state model that is excited via an external light source. This system can be represented via the following Hamiltonian:

$$\hat{H} = \hat{H}_0(r) + \hat{V}(t) \tag{2.1.1}$$

This Hamiltonian is clearly split into two separate parts, wherein $\hat{H}_0$ is the time independent term that represents the unilluminated ground state atom. With $\hat{V}$ representing the time-dependent term that represents the interaction between the incident electromagnetic field and the ground state atom. Given this our next step is to solve the Schrödinger equation:

$$\hat{H}\psi_i = i\hbar\frac{\partial\psi_i}{\partial t} \tag{2.1.2}$$

This is first order ordinary differential equation, which has the following solutions:

$$\psi_i(r,t) = \sum_{i=1}^{2} c_i\psi_i(r)e^{-\frac{iE_it}{\hbar}} \tag{2.1.3}$$

Wherein:

- $\psi_i(r)$ represents the maximum radial contribution of the atom relative to its distance from the nucleus
- $c_i(t)$ is a constant governed by the time-dependent portion $\hat{V}$
- And E_i represents energy of the i-th level

To determine the constants for the system, we can take the above wavefunction and substitute it back into the time-dependent Schrödinger equation:

$$c_1\hat{V}\psi_1 e^{-\frac{iE_1t}{\hbar}} + c_2\hat{V}\psi_2 e^{-\frac{iE_2t}{\hbar}} = i\hbar\dot{c}_1\hat{V}\psi_1 e^{-\frac{iE_1t}{\hbar}} + i\hbar\dot{c}_2\hat{V}\psi_2 e^{-\frac{iE_2t}{\hbar}} \quad (2.1.4)$$

We can then take the expectation value for this system which involves multiplying it by a complex conjugate, integrating over all space, and recalling the orthonormality of states. This leaves us with the following:

$$\dot{c}_1 = -\frac{i}{\hbar}(c_1\hat{V}_{11} + c_2\hat{V}_{12}e^{-i\omega_0 t}) \quad (2.1.5)$$

$$\dot{c}_2 = -\frac{i}{\hbar}(c_1\hat{V}_{21}e^{i\omega_0 t} + c_2\hat{V}_{22}) \quad (2.1.6)$$

Wherein:

- The energy separation between the two states is: $E_2 - E_1 = \hbar\omega_0$
    - With $\omega = \omega_0 + \delta\omega$ - The assumption that the incident light, $\delta\omega$, is extremely close to resonance
- $\hat{V}_{ij} = \int \psi_i^* \hat{V}(t)\psi_j \, \mathrm{d}^3r = \langle i|\hat{V}(t)|j\rangle$ the ij'th matrix element of $\hat{V}(t)$, upon calculating the expectation value

This gives us two first order ordinary differential equations with respect to the constants. However, this does not give us much information. We can make this even more concrete by considering the following understanding the effect an electric field has on the energy of an atomic dipole:

$$\hat{V}(t) = e(r \cdot \varepsilon(t)) \tag{2.1.7}$$

Wherein:

- e is the electric charge
- r is the direction of polarization
- $\varepsilon(t)$ is the electric field

For which we can choose to align the polarization of the electric field along the x-axis for simplicity results in the following:

$$\hat{V}(t) = ex\ \varepsilon_0 \cos(\omega t) \tag{2.1.8}$$

The individual matrix elements can be found as follows, by finding the expectation value:

$$\hat{V}_{ij} = \frac{e\varepsilon_0}{2}(e^{-i\omega t} + e^{i\omega t}) \int \psi_i{}^* x \psi_j \, \mathrm{d}^3 r \tag{2.1.9}$$

For which we make a simple substitution:

$$\mu_{ij} = -e \int \psi_i{}^* x \psi_j \, \mathrm{d}^3 r \tag{2.1.10}$$

Thus, we are left with:

$$\dot{c}_1(t) = i\frac{\varepsilon_0\mu_{12}}{2\hbar}(e^{i(\omega-\omega_0)t} + e^{-i(\omega+\omega_0)t})\, c_2(t) \tag{2.1.11}$$

$$\dot{c}_2(t) = i\frac{\varepsilon_0\mu_{12}}{2\hbar}(e^{-i(\omega-\omega_0)t} + e^{+i(\omega+\omega_0)t})\, c_1(t) \tag{2.1.12}$$

Wherein the Rabi frequency is defined as:

$$\Omega_R = \frac{\varepsilon_0\mu_{12}}{\hbar} \tag{2.1.13}$$

2.1.2 The Idealized Scenario

Suppose instead we excited the system resonantly, i.e. $\omega = \omega_0$, that is to say it is excited with the same energy as the transition between the ground and excited states. We would find that the system would reduce to:

$$\dot{c}_1(t) = \frac{i}{2}\Omega_R c_2(t) \tag{2.1.14}$$

$$\dot{c}_2(t) = \frac{i}{2}\Omega_R\, c_1(t) \tag{2.1.15}$$

Having simplified our system, we can actually solve this by differentiating one of the equations to get a second order ordinary differential equation. Which has the following solution:

$$c_1(t) = \cos\left(\frac{\Omega_R t}{2}\right) \tag{2.1.16}$$

$$c_2(t) = i\sin\left(\frac{\Omega_R t}{2}\right) \tag{2.1.17}$$

This solution is clearly oscillatory. Notice that the frequency of oscillation is $\frac{\Omega_R}{2\pi}$, this is the frequency at which the electron population oscillates from the excited to ground states. This is an astounding

result that simply falls out from the theory. However, it highly idealistic. What if we were to consider more realistic parameters?

2.1.3 Approaching the Real World

Rabi oscillations are difficult to observe in the lab frame, due to damping effects within the system as well as the surrounding environment. While there may be many reasons, we can consider two well defined mechanisms that may contribute damping.

The first of which is called longitudinal relaxation 'T_1;' which is due to the probabilistic nature of electron decay. This process can be modelled as a Gaussian distribution, with an average number of spontaneous emissions occurring at the radiative lifetime. If not accounted for, when undergoing Rabi oscillations, spontaneous emission has the potential to break the Rabi cycle. To account for this, the radiative lifetime sets the upper limit for the rabi cycle, thus the period of rabi cycle must fall within this radiative lifetime. Despite this consideration, as the radiative process is probabilistic, spontaneous emission may still occur.

The second mode of damping is called transverse relaxation 'T_2.' While the above process is governed by the atom itself, here the environment causes damping instead. If the atom, while in an excited state, were to undergo elastic or inelastic collisions, this can change the wavefunction of the atom. While the frequency and the intensity are untouched, a more subtle change in the wavefunction's phase occurs. This change in phase has the potential to destroy the Rabi oscillations. While the terms Poissonian and sub-Poissonian will be described in further detail in the next section. Suffice to say that

a simple way to understand this is that the Rabi phenomenon is observed under sub-Poissonian conditions, which have very little deviation from the average. Given that Poissonian light is coherent light, which preserves frequency and phase, the more stringent sub-Poissonian light must also preserve the frequency and phase. Thus any change in phase will result in a decrease in coherence, which can result in the destruction of the Rabi cycle.

It is interesting to note that while these phenomena are, to my knowledge, unrelated, there is a way to relate the two in an equation:

$$\frac{1}{T_2} = \frac{1}{2T_1} + \frac{1}{T_2^*} \tag{2.1.18}$$

Wherein T_2^* star is called the overall decoherence and is considered the overall dephasing of the system. Given this, we can now modify equation (2.1.17), to include damping effects. Suppose we consider that overall damping rate is 'gamma,' and it primarily affects the probability that the electron is in the upper level. We can make the following considerations:

- $\xi = \frac{\gamma}{\Omega_R}$
- $\Omega' = \Omega_R\sqrt{4 - \xi^2}$

This results in the following equation:

$$|c_2(t)|^2 = \frac{1}{2(1+2\xi^2)}\left[1 - \left(cos(\Omega' t) + \frac{3\xi}{\sqrt{4-\xi^2}} sin(\Omega' t)\right) e^{-\frac{3\gamma t}{2}}\right] \tag{2.1.18}$$

While hard to believe, this does indeed reduce to equation 2.1.17 when $\gamma = 0$. This result is often used in experimental modelling to confirm the presence of dampened Rabi oscillations. It is my hope in this

thesis, that I will be able to improve upon this model so that it better fits the experimental results found by the Reimer group.

One can verify the quantum nature of a system by the presence of Rabi oscillations, however there is no way, at present, to observe electron dynamics. However, one can observe the emissions from the electrons which also follow the Rabi cycle. To get a better picture of this, it is important to understand the framework used to understand photons, which will be considered in the next section.

2.2 Object Studied – The Photon

While it is understood that Rabi oscillations represent the change in electron populations as they oscillate between the ground and excited states; we are unable to directly study this in any meaningful way. However we are able to learn from the by-product of these oscillations, photon emission, as these emissions still fall under the Rabi cycle. To understand this we must understand that light coming from a quantum source is special and makes it conducive to studying these effects.

Under a classical lens, we think of light as a wave, a steady stream of photons. That is to say that we can depend on photons being present at regularly spaced time-intervals. However, photon production is a highly probabilistic process. How do we reconcile these two understandings?

The probabilistic process that governs photon production is said to be Poissonian, which can then be further broken into 3 categories: Super-Poissonian, Poissonian, and Sub-Poissonian. But

these words on their own have little meaning, so let's consider a toy model (Fox, 2006) for some context.

2.2.1 The Toy Model

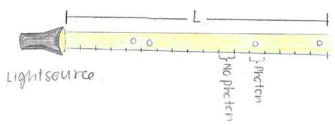

Figure 2.2.1: Toy Model

Suppose we consider a coherent beam of light with length L which contains n photons. With coherence defined as light whose photons oscillate with the same frequency and are in phase with one another. We can divide this beam into smaller segments of the same size, and we can do so until we have infinitely many of these identical segments. What we will find is that the probability of finding a photon within a given segment is extremely small. Now suppose we consider the entire length of the beam instead. What is the likelihood of finding n sections containing a photon in a beam of length L with N sections? We can do this by considering a binomial distribution, this looks as follows:

$$P(n) = \frac{N!}{n!\,(N-n)!} p^n (1-p)^{N-n} \qquad (2.2.1)$$

Wherein

- N total number of sections
- n number of successes – finding a section with a photon
- $p = \frac{\overline{n}}{N}$ probability of success, can also be defined as the average photon count divided by the total number of sections

This can be understood piecewise. The first term, the quotient, represents the number of ways one can select n, i.e. segments with photons, out of N segments. Wherein $N - n$ represents the number of

segments with zero photons. We then multiply this by the probability of getting a segment with a photon, i.e. p^n, and $N-n$ failures, i.e. $(1-p)^{N-n}$. The entirety of this product gives us the probability of finding n segments containing one photon. We can rewrite this by considering the average number of photons within a beam of length L:

$$P(n) = \frac{N!}{n!\,(N-n)!}\left(\frac{\bar{n}}{N}\right)^n \left(1-\frac{\bar{n}}{N}\right)^{N-n} \tag{2.2.2}$$

As the beam length is large, N is taken to be infinitely large. Thus, we can then use Stirling's approximation for the first part of equation 2.2.2:

$$\lim_{N\to\infty}(lnN!) = NlnN - N \tag{2.2.3}$$

Along with the binomial theorem

$$(1+x)^n = 1 + nx + \frac{n(n-1)}{2!}x^2 \ldots . = \tag{2.2.4}$$

We can combine the above considerations to rewrite equation (2.2.2):

$$P(n) = \frac{\bar{n}}{n!}e^{\bar{n}} \tag{2.2.5}$$

The resultant equation is defined as the Poisson distribution. We can take special note of how this equation is characterized by the mean, $\bar{n}$, which is unique to a Poisson distribution. In fact, the standard deviation is given as follows:

$$\Delta n = \sqrt{\bar{n}} \tag{2.2.6}$$

Now that we have established what it means to have a Poissonian distribution, the other classes are simple to understand. They are as follows:

Classification of Light	What that Means	
Sub-Poissonian	$\Delta n < \sqrt{\bar{n}}$	Wherein Δn is the standard deviation
Poissonian	$\Delta n = \sqrt{\bar{n}}$	
Super-Poissonian	$\Delta n > \sqrt{\bar{n}}$	

Figure 2.2.2 Classifications of light

We can further understand these classifications by considering them under physical contexts. We have defined Poissonian light as that which is coherent light. This has a standard deviation that is the square-root of the mean. This light is characterized by constant frequency, phase, and intensity. Suppose we were to vary the intensity over time. We would find that the number of photons falling within one standard deviation of the mean would be larger than that of coherent light. This results in super-Poissonian light, examples of this are thermal light and black body radiation.

Based on what we have above, we can then understand that sub-Poissonian light has a narrower distribution. In an idealized situation, we can assume that each segment used in the Poissonian light has a single photon with certainty. Thus the number of photons found in a time T, would be exactly the number of subsegments. Our standard deviation would be zero. This sounds like a deterministic source, rather than the probabilistic model encapsulated by light. But what is characterized by this? A perfectly coherent beam is the most stable light in classical optics; thus we must consider a non-classical source, a quantum source.

This sounds rather mythical, however there are many sources of sub-Poissonian light. There are four broad classes (Davidovich, 1996):

Type	Examples
Atom is passive, playing a nonlinear refraction index	Parametric processes and second-harmonic generation
Atom is active, exchanging energy with the field	Atomic fluorescence and sub-Poissonian lasers
Simultaneous emission of two nondegenerate photons	Parametric processes and two-photon lasers
Noise reduction from measurement	Continuous system measurement to prevent fluctuations

Figure 2.2.3 Classifications of Sub-Poissonian light

The source used in this thesis will be the quantum dot, which is an example of the second (single photons) and third classes (entangled photons). Further understanding for this is given in the next section.

2.3 Production of Object – The Quantum Dot

In order to study photons, one needs a source for them, and in particular, a deterministic source. As mentioned previously, if we consider an idealized sub-Poissonian system for each section, instead of a chance, there would be a guaranteed photon. In essence, a deterministic source. In this section we will consider in depth the source used in this experiment: the quantum dot.

First synthesized by Alexey Ekimov, Allen J. Bard, and Louis E. Brus in 1981, the quantum dot was created in order to address dependence on fossil fuels and shift towards solar energy

conversion. This quantum dot was created via the placement of a semiconductor within a glass matrix. The semiconductor used was lead (II) sulfide (PbS), and it was noticed that while bulk PbS is black, the matrix exhibited an array of colours that were dependent on the size of the semiconductor. In the next section, we will consider an overview of the structure and mechanism of the quantum dot.

2.3.1 Quantum Dot Structure and Mechanism – Core-Shell Quantum Dot

There are at least three possible structures for quantum dots, and we will focus on the core-shell structure in this thesis. The general structure of this quantum dot is a semi-conductor coated with another substance. The other substance must have a bandgap that is higher than that of the semiconductor. In effect, creating a confining potential; the presence of which creates a spectrum of bound states.

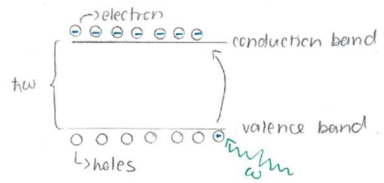

Figure 2.3.1- Bandgap of ħω

Before we continue, I want to further elaborate on the language used above. Any solid can be characterized as having a valence band – wherein the electrons are bound to the atom and a conduction band wherein in the electrons are excited and free and not bound to the atom. The bandgap is an intermediate section within which there are no electronic states. In the quantum dot structure given above, the quantum dot alone would have infinitely (theoretically) many states accessible in the conduction band. Coating this with a second material with a higher bandgap,

creates a maximum potential for the electron to achieve, effectively confining it. This confining potential then serves to create a spectrum of bound states. The use of a confining potential to create bound states mimics the mechanisms in an atom and as such the quantum dot is also called an artificial atom.

Figure 2.3.2 Core-Shell Quantum Dot Structure

One of the reasons for the popularity of the quantum dot is in its ability to create entangled pairs. However, I am getting ahead of myself, let us consider a simple ground to excited state model. In order to create a photon in this system, one must excite an electron from the valence band into the conduction band. This creates a hole that the electron leaves behind in the conduction band which can be treated like a particle. When the electron relaxes from the excited state to the hole in the ground state, it emits a photon with the same energy between the excited and ground states. This process is called radiative recombination. An ideal quantum dot will only allow for a select number of electron-hole pairs to exist, thus controlling the number of photons emitted.

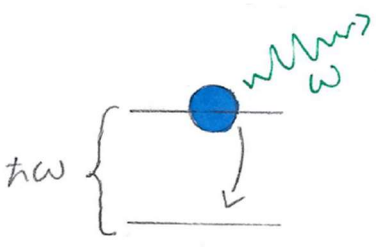

Figure 2.3.3 Radiative Recombination

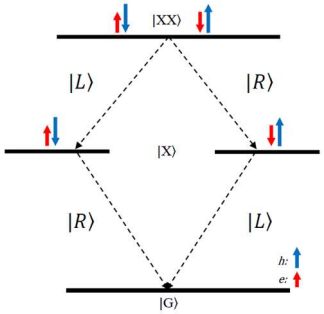

Figure 2.3.4 - Biexciton-Exciton Cascade (Ahmadi,2019)

However as mentioned previously, one of the reasons for the use of the quantum dot is in its ability to produced entangled pairs. It does this via a secondary excited state – the bi-exciton. The biexciton is a collection of two electron and hole pairs, which have the opposite angular momentum and undergo two recombinations. This system is not unlike the filled s-shell of an atom further motivating the name

'artificial atom.' Suppose upon the first recombination, the biexciton transition, we generate a left circularly polarized photon (LCPP) and the remaining electron-hole pair. Upon the second, the exciton transition, the remaining pair will recombine and emit a right circularly polarized photon (RCPP). Similarly, if the biexciton transition results in an RCPP and electron hole pair, then the exciton transition will result in a LCPP. This pathway is called the Biexciton-Exciton Cascade and is fundamental in the creation of entangled pairs. In an idealized case, it is impossible to determine which path the transition will take, and as such we end up with a superposition state. This is also a Bell state, indicating that it is a state of maximal entanglement (Ahmadi, 2019), which is seen below:

$$|\Psi\rangle = \frac{1}{\sqrt{2}}(|RL\rangle + |LR\rangle) \qquad (2.3.1)$$

While entanglement will not be an element discussed in this thesis, the need for a secondary excited state, a third state in total, adds an element of difficulty to the model. As mentioned in section 2.1, Rabi oscillations are often modelled in two-state systems.

We have spoken at length about radiative recombination and how it is leveraged to create entangled pairs in the biexciton cascade. But how do we excite the electron to begin with? There are several excitation schemes used to excite the quantum dot, but we will pay particular focus to the Two-Photon Resonant Excitation (TPE) scheme.

Prior to the TPE scheme, off-resonant excitation was the main scheme used to excite quantum dots. In this excitation scheme, energy far above the bandgap is applied to the quantum dot. The electron relaxes into the first excited state via phonon interactions. Phonons are vibrations that can be treated as particles – quasi-particles. It is then able to recombine with its constituent hole and emit

light. However, due to the lack of specificity of this technique, the likelihood of multi-photon emission occurring is high which can lead to broadening in the emission lines.

Multi-photon emission is not the only problem caused due to off-resonant excitation, but it is one of the challenges that motivated the development of the TPE scheme. The premise of this scheme is to apply a laser pulse to the quantum dot with an energy equal to:

$$\frac{E_{Biexciton} - E_{Ground}}{2} \qquad (2.3.2)$$

This energy lies between the biexciton and exciton transition energies. The key to this excitation scheme is in that it does not resonantly excite the biexciton directly. The biexciton is like a filled s-shell with two electrons with opposing angular momenta, thus a net spin of 0. Therefore an excitation with a photon, which has a spin of 1, would violate the Pauli exclusion principle as the net angular momentum would not sum to 0. To avoid this we can use two photons to excite the biexciton instead. By bombarding the quantum dot with a laser of the energy given above, the likelihood that two photons would be able to excite biexciton is extremely high, resulting in an excitation that does not violate the exclusion principle (Ahmadi, 2019).

With this we have detailed the structure of the quantum dot as well as the mechanisms governing the production of photons with the quantum dot. We are now able to detail the quantum dot parameters used by the Reimer group as well as in this thesis.

2.3.2 Quantum Dot Used in Thesis

With the appreciable context provided above, we can further delve into the quantum dot parameters used in this thesis. The Reimer group quantum dot is composed of a wurtzite InP nanowire with a tapered edge along with an optically active InAsP section. The nanowire facilitates the transition the emitted photon from the quantum dot to the external environment adiabatically (transition over a long enough time period that edge effects are nonexistent). This means that it serves to reduce the chance for total internal reflection and allows for maximum transition. The quantum dot is composed of Indium (Group V) and Phosphide (Group III); thus this quantum dot is composed with a III-V semiconductor. The laser used to excite this quantum dot is the Coherent Mira 900 Ti: Sapphire laser with energy 894.0 nm. The biexciton emission are peaked at 894.6 nm and the excitation emissions are peaked at 893.3 nm.

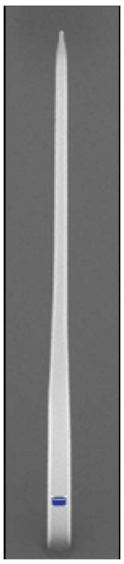

Figure 2.3.5 – Reimer group Quantum dot. InP Nanowire, and optically active InAsP highlighted in blue (Ahmadi, 2019)

We have established the context underlying the production of the photon – the quantum dot, along with the particular parameters that would be considered in this thesis. We can now establish the mathematics used model to Rabi oscillations from photon emissions produced by the quantum dot.

2.4 Lindblad Master Equation

In physics, there are multiple formalisms used to define the make up of a system, one of which is the Hamiltonian. This takes the Lagrangian formalism, which takes the difference between the kinetic and potential energies, and performs a Legendre transforms. This takes the input configuration space co-ordinates of co-ordinate and velocity and maps them onto the phase space co-ordinates for position and momentum. Without getting into the minutiae of this transform, we can understand that this transform results in an equation that represents the total energy of the system.

However, this understanding only considers the system itself. While many important findings and results can be derived from this approximation, it can be far from an accurate representation of reality. Enter the Linblad master equation, which is touted as a more generalized version of the Hamiltonian. Not only does this consider the system's dynamics, but also the environmental effects and whatever mechanism that couples one to the other.

So how does one do this? We map the system, the environment, and their coupling onto a space with some careful consideration. In our case, we map our systems onto the Hilbert space. This Hilbert space is a complex vector space that is

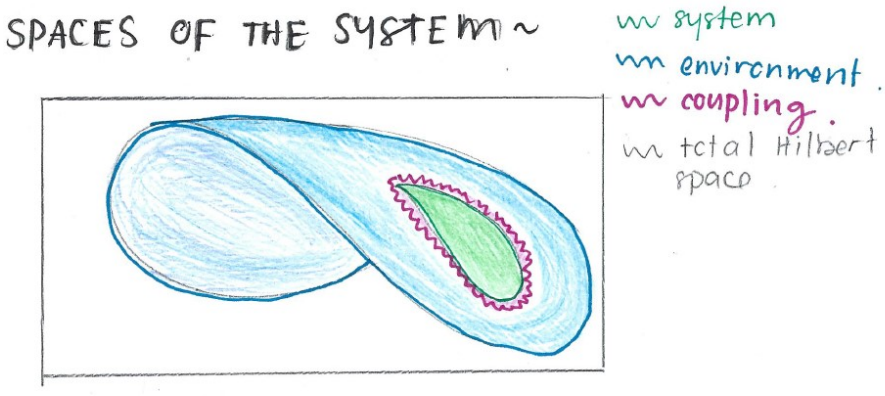

Figure 2.4.1 Total Set of Hilbert Spaces

equipped with an inner product. This space is spanned by a set of basis vectors, from which we can construct the entire space. In the example of the quantum dot, the levels of excitation are used to map the system. One can map the system, the environment and the coupling using separate Hilbert spaces. The total Hilbert space is then (Manzano, 2020):

$$H_{Total} = H_{System} \otimes H_{Environment} \otimes H_{Coupling} \tag{2.4.1}$$

As we are dealing with a quantum dot system, we will use the same basis states to define the environment and the coupling. This is made possible under the understanding that any state can be written as a linear combination of alternate basis states. This is written mathematically as:

$$|a\rangle = \sum_i \beta_i |b_i\rangle \tag{2.4.2}$$

Wherein

- β_i are complex coefficients
- $|b_i\rangle$ are the basis states in an alternate basis

It is key to understand that while these use the same language, i.e. the same basis states, the system, environment, and coupling belong to separate Hilbert spaces, and as such the basis states are separate as well. We are just able to translate each system into a single language, to gain a better understanding of the what we have.

We are able to manipulate this Lindblad master equation, similar to how we would a regular Hamiltonian, such that we can extrapolate information of all possible trajectories for a system. Suppose we wanted to understand the progression of the system coupled to a given environment. We can intuit this by considering the following equation:

$$\dot{\rho} = -\frac{i}{\hbar}[H, \rho] \tag{2.4.3}$$

In plain terms, we can represent our system by a density matrix. This contains all the relevant information of the system under the basis of the Hilbert space. Its progression over time, i.e., $\dot{\rho}$, can be defined under the Heisenberg picture as the commutation relationship between the Hamiltonian and the system's density matrix. Solving this equation grants us the equations of motion for our system, and as such gives us information about the progression of the system. This process is the quantum analogue for the Poisson bracket, which is used to derive equations of motion from a given Hamiltonian.

While the Heisenberg picture is equivalent to the Schrödinger picture under the Stone-von Neumann theorem, and as such realize the same results. However, the inclusion of the environment and coupling is easier under the Heisenberg picture and looks as follows:

$$\dot{\rho} = -\frac{i}{\hbar}[H, \rho] + \sum_i \gamma_i \left({\mathcal{L}_i}^\dagger \rho \mathcal{L}_i - \frac{1}{2}\{{\mathcal{L}_i}^\dagger \mathcal{L}_i, \rho\} \right) \tag{2.4.4}$$

Wherein:

- ${L^\dagger}_i$ and L_i are collapse operators and represent the interaction between the system and the environment.
- γ_i is the rate of spontaneous emission due to the collapse operators (Fischer, Dynamical Modeling of Pulse Two-Photon Interference, 2016)

This inclusion of the environment as well as the coupling, defining the interaction between the two, is a picture that is more grounded in reality. As such, this has the potential to provide further

insight and predictive capabilities to any model using it. It is this consideration that governs the technique used in this thesis.

-

Now that we have established context for the parts used in the building of this model, it's now time to put it work for some usable results, which follow in the next chapter.

Chapter 3 – Methodology, Findings, and Analysis

Having established an understanding for the context motivating this thesis, we can now establish and utilize the model in this chapter. We will do this by going through the methodology behind the model as well as a thorough analysis of its results output by this model. To reiterate the purpose, we seek to create a model that is better able to account for environmental dephasing effects that lead to dampening in the Rabi oscillations from a quantum dot source.

3.1 General Methodology

This project was started under the guidance of Ph.D. candidate Matteo Pennacchietti. He had acquired some experimental data for detecting Rabi oscillations. In order to confirm his findings, he used equation (2.1.18) to fit his data, which can be seen in figure 3.1.

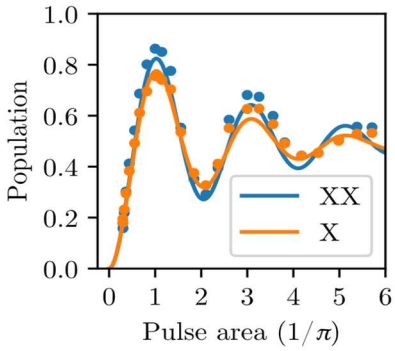

Fig 3.1.1 Experimental data of Matteo Pennacchietti with Rabi Oscillation fit from equation (2.1.18)

As we can see, this a rather close fit to the data he found. However, ever the perfectionist, he wondered if there was any way to get a better fit. It was suggested that including a better description for environmental dampening effects would give a curve that was more aligned with the data. With this idea, he suggested the following paper: Coherence and Degree of Time-Bin Entanglement from Quantum Dots, by authors Tobias Huber, Laurin Ostermann, Maximilian Prilmüller, Glenn S. Solomon, Helmut Ritsch, Gregor Weihs, and Ana Predojević. This is be discussed further in the next section.

3.1.1. Motivation

Huber et al. sought to optimize the laser pulse used to reduce laser induced dephasing and increase the exciton population probability not from direct excitation, but rather from biexciton decay instead. While the method of entanglement used is different from that used by Matteo (Time-Bin entanglement vs. Polarization), nonetheless the effective Hamiltonian and Liouvillian used in this paper are general enough to be used for our purposes as well. The Hamiltonian is as follows:

$$H = \frac{1}{2}\left(\Omega_1(|g\rangle\langle x| + |x\rangle\langle g|) + \Omega_2(|b\rangle\langle x| + |x\rangle\langle b|)\right) + +(\Delta_x - \Delta_b)|x\rangle\langle x| - 2\Delta_b|b\rangle\langle b| \quad (3.1.1)$$

Wherein:

- Ω_i are the Rabi frequencies of the ground-biexciton and ground-exciton coupling. In our case $\Omega_1 = \Omega_2$
- $|g\rangle, |x\rangle, |b\rangle$ are the basis states for the quantum dot. They are ground, exciton, and biexciton respectively
- Δ_x difference between intermediate transition state and the exciton

- Δ_b detuning due to intermediate state between biexciton and ground state, in this case 0 due to resonant excitation

And the following Liouvillian (Collapse Operators):

$$\mathcal{L}_1 = \frac{\gamma_b}{2}|b\rangle\langle x| \tag{3.1.2}$$

$$\mathcal{L}_2 = \frac{\gamma_x}{2}|x\rangle\langle g| \tag{3.1.3}$$

$$\mathcal{L}_3 = \frac{{\gamma_{bx}}^{dephasing}}{2}(|b\rangle\langle b| - |x\rangle\langle x|) \tag{3.1.4}$$

$$\mathcal{L}_4 = \frac{{\gamma_{xg}}^{dephasing}}{2}(|x\rangle\langle x| - |g\rangle\langle g|) \tag{3.1.5}$$

Wherein:

- $\mathcal{L}_1$ and $\mathcal{L}_2$ represent population loss due to spontaneous decay
- γ_b and γ_b represent the dephasing rates for the biexciton and exciton respectively
- $\mathcal{L}_3$ and $\mathcal{L}_4$ represent the dephasing between the biexciton and exciton and exciton and ground respectively
- ${\gamma_{bx}}^{dephasin}$ and ${\gamma_{xg}}^{dephasing}$ represent the dephasing rates between the biexciton and exciton and exciton and ground respectively

Thus we can determine the evolution of the system defined as $\dot{\rho}$, which follows the Linblad Master Equation:

$$\dot{\rho} = -\frac{i}{\hbar}[H, \rho] + \sum_i \gamma_i \left(\mathcal{L}_i{}^\dagger \rho \mathcal{L}_i - \frac{1}{2}\{\mathcal{L}_i{}^\dagger \mathcal{L}_i, \rho\} \right) \quad (3.1.6)$$

As we can see, solving this system analytically is quite the challenge? So how do we go about overcoming this?

3.1.2 General QuTiP Implementation

There are multiple powerful pieces of software that would allow me to solve the above system, however QuTiP jumped out as an opportunity to learn something new, but also for its user friendliness. QuTiP is a Python package that has several tutorials available for one to become accustomed to it. As well, this package is easily implementable as the analytic work is done within the package, with one's only job being to input the required information.

As Lindblad Master Equation approach was proposed, the master equation solver program, that is readily available on QuTiP, was used to create our model. This required the following parameters:

- The Effective Hamiltonian
- Wave function: Providing information on the initial state of the system
- Gaussian pulse used to excite the system
- Tlist: A list of times that are used to perform calculations
- A Set of Collapse Operators: Which detail dephasing within the system
- and a Set of Environmental Operators: Which detail dephasing due to environmental factors

Upon submitting these parameters, we are able to calculate the emission probabilities, as per the following expectation value:

$$P_i(t_f) = \int_0^{t_f} \langle i|\hat{\rho}(t)|j\rangle \; dt \qquad (3.1.7)$$

Which we can then plot for results and further analysis.

Now that we have detailed the general process behind implementing the model on QuTiP, let us consider how this worked with our specific system.

3.2 Implementation, Findings, and Analysis

3.2.1 Challenges

Of course, if the problem was as easy to solve as above, we wouldn't have much of a problem to work with. However, due to the nature of the system in question, there were some challenges which needed to be solved in order for the model to be successful.

- This was 3-level System rather than a 2-Level System
- Assigning operators that were usable under a QuTiP framework
- The Pulse Shape interfering with the detection of Rabi Oscillations

However, despite these challenges, a model was created that could be fine-tuned to generate usable results.

Challenge 1 – Dealing with a 3 Level System

The first challenge addressed was that we were dealing with a three-level system, rather than a two-level system, so we needed to be careful assigning the typical raising and lowering operators. To address this we considered the following question: Was it possible to construct SU(2) in terms of 3×3 matrices? Or put more simply, is possible to construct 3-D Pauli matrices? Following the framework provided by (reductionista, 2016), we can create 3-D Pauli matrices by starting with the idea of how the 3-D raising and lowering operators would work.

Suppose we consider the $S_z$basis, we know what we want when we apply raising and lowering operators on these eigenstates, which look as follows:

$$S^- \begin{bmatrix}1\\0\\0\end{bmatrix} = \begin{bmatrix}0\\1\\0\end{bmatrix}, S^- \begin{bmatrix}0\\1\\0\end{bmatrix} = \begin{bmatrix}0\\0\\1\end{bmatrix}, \text{and } S^- \begin{bmatrix}0\\0\\1\end{bmatrix} = 0 \qquad (3.2.1)$$

$$S^+ \begin{bmatrix}1\\0\\0\end{bmatrix} = 0\ , S^+ \begin{bmatrix}0\\1\\0\end{bmatrix} = \begin{bmatrix}1\\0\\0\end{bmatrix}, \text{and } S^+ \begin{bmatrix}0\\0\\1\end{bmatrix} = \begin{bmatrix}0\\1\\0\end{bmatrix} \qquad (3.2.2)$$

This results in the following matrix representation of the raising and lowering operators:

$$S^- = \begin{bmatrix}0 & 0 & 0\\1 & 0 & 0\\0 & 1 & 0\end{bmatrix} \text{ and } S^+ = \begin{bmatrix}0 & 1 & 0\\0 & 0 & 1\\0 & 0 & 0\end{bmatrix} \qquad (3.2.3)$$

From this, we can easily determine all other operators by considering the following relationships:

$$S_x = \frac{1}{2i}(S^+ + S^-) \; and \; S_y = \frac{1}{2i}(S^+ - S^-) \tag{3.2.4}$$

$$[S_x, S_y] = i\hbar S_z \tag{3.2.5}$$

We now have a representation that is easily implementable in QuTiP, however, this is where we encounter our next challenge: How to assign raising and lowering operators found in this section given the format of the effective Hamiltonian given in the paper.

Challenge 2 – Assigning Operators

Given that we have established what operators must be used, we do not know how they compare to the operators of the effective Hamiltonian. However we can consider the material in Dr. Michal Bajcsy's ECE 770 (Bajcsy, 2022) notes for guidance in this matter. On slide 11, he suggests the following transformations:

$$S^- = |x\rangle\langle g| \text{ and } S^+ = |g\rangle\langle x| \tag{3.2.6}$$

Assuming that this can also be used in a three-dimensional basis this leaves us with the following:

$$S_{gx}{}^- = |g\rangle\langle x| = \begin{bmatrix} 0 & 0 & 0 \\ 0 & 0 & 0 \\ 0 & 1 & 0 \end{bmatrix} \tag{3.2.6}$$

$$S_{xb}{}^- = |x\rangle\langle b| = \begin{bmatrix} 0 & 0 & 0 \\ 1 & 0 & 0 \\ 0 & 0 & 0 \end{bmatrix} \tag{3.2.6}$$

$$S_{gx}{}^+ = |x\rangle\langle g| = \begin{bmatrix} 0 & 0 & 1 \\ 0 & 0 & 0 \\ 0 & 0 & 0 \end{bmatrix} \tag{3.2.6}$$

$$S_{xb}{}^+ = |b\rangle\langle x| = \begin{bmatrix} 0 & 1 & 0 \\ 0 & 0 & 0 \\ 0 & 0 & 0 \end{bmatrix} \tag{3.2.6}$$

These sum to get the total raising and lowering operators in equation 3.2.3. With this we have now established the relevant operators for this problem and are now able utilize QuTiP. However, upon implementation we run into our final challenge.

Challenge 3 – Addressing the Pulse Shape

Now for the final challenge, and perhaps the hardest one, addressing the pulse shape of the incident laser. The Ω of equation (3.1.1) is a parameter that represents the shape of the incident laser pulse. Initially we used the parameters defined in the QuTiP tutorial for two-photon interference:

$$\Omega(t) = \frac{\Omega}{2} e^{\frac{-(t-t_0)^2}{2{t_p}^2}} \tag{3.2.7}$$

Wherein:

- Ω is the max. intensity of the pulse
- t_p is the standard deviation of the pulse

However, this just resulted in the following:

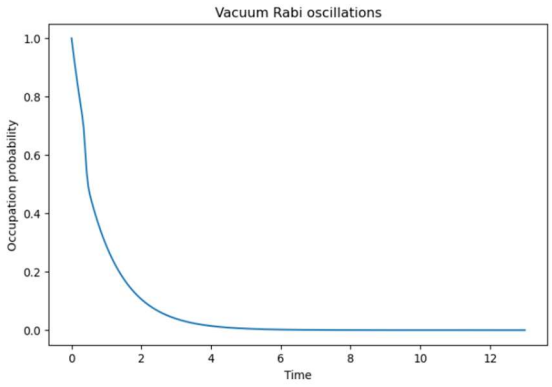

Figure 3.2.1 – Initial Rabi Oscillation curve

A typical decay curve with no Rabi oscillations. So how do we address this? Unfortunately, unlike the above challenges, there were no formulae or theorem, so we had to use the tried-and-true trial and error method. The only consideration kept in mind was that this needed to follow a short pulse regime, that is to say that the Ω must be greater than the standard deviation t_p. When t_p is the same order of magnitude as Ω, we finally get Rabi oscillations, the results of which follow in the next section.

3.2.2 Results and their Analysis

Having solved the above challenges, we end up with the following parameters used to determine this model are as follows:

- The Effective Hamiltonian –

$$H = \frac{\Omega(t)}{2}\left({S_{gx}}^{+} + {S_{bx}}^{+} + {S_{gx}}^{-} + {S_{bx}}^{-}\right) + 0.1\left({S_{bg}}^{\dagger} S_{bg}\right) \qquad (3.2.8)$$

  - Wherein $\Delta_x = 0.1$

- Gaussian pulse (Equation (3.2.7)) used to excite the system –

$$\Omega(t) = \frac{19.40}{2} e^{\frac{-(t-0.2025)^2}{2(10)^2}} \qquad (3.2.9)$$

  Wherein

  - $t_0 = 0.2025s$
  - $t_p = 10s$
  - $\Omega = 19.40$

- Wave function: Providing information on the initial state of the system – Ground state of Harmonic oscillator system

Upon running this code we end up with the following plots for the ground, exciton, and biexciton populations:

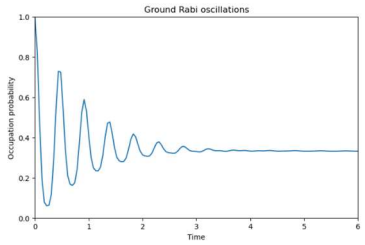

Figure 3.2.2.1 - Ground State Rabi Oscillations with time in s

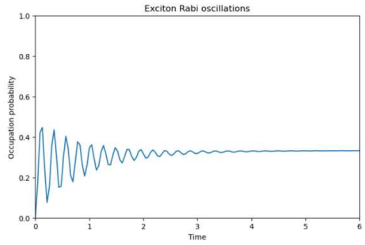

Figure 3.2.2.2 – Exciton State Rabi Oscillations with time in s

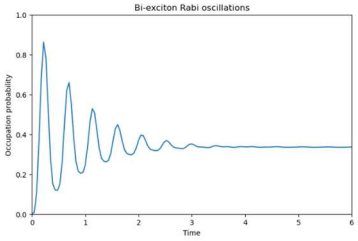

Figure 3.2.2.3 – Bi-exciton State Rabi Oscillations with time in s

From which we can see the presence of Rabi oscillations, suggesting that we have created a successful model for Rabi oscillations.

Let us consider these results carefully. Beginning with the ground state population. As we would expect, initially before t_0, 100% of the population would be in the ground state. As time progresses and the peaks level out, we notice that the population of the ground state oscillates about the 35% probability of occupation. In contrast the biexciton and exciton populations start at 0 until t_0. Upon which the biexciton population reaches just under 90% probability of population, and the exciton population reaches just under 50% probability of population. This suggests that the dephasing mechanisms implemented via the Hamiltonian allow for direct exciton population as a means for dephasing. As the peaks in the biexciton and exciton diminish, we notice that over time these populations also oscillate at about 35% occupation, similar to the ground state population.

While these results are extremely promising, they are preliminary as there are further challenges that need to be addressed before this can be used as a fitting model for experimental data. This will be further discussed in the conclusions and future considerations of this thesis.

Chapter 4 – Conclusions and Future Considerations

The purpose of this thesis was to determine the quantum nature of the quantum dot through the detection of Rabi oscillations. In order to do so, our first order of business was to establish what the Rabi oscillation was. It was determined that the frequency of oscillation for a system with Rabi oscillations could be detected from solving the Schrödinger equation with the Hamiltonian of a ground state atom interacting with an electric field. Upon further simplification by the means exciting the atom resonantly, we found that the Rabi oscillation was found in the arguments of equation 2.1.16 and 2.1.17, suggesting a frequency of oscillation of $\frac{\Omega_R}{2\pi}$. However, here we also learned that the system can be prone to dephasing due to a probabilistic light source, and as such can be broken before observation. Thus our next order of business was to establish a deterministic light source.

In section 2.2 we quantified the statistical nature of light. What we found was that light generally followed a Poissonian distribution. However a sub-Poissonian distribution under idealized conditions could be considered a deterministic source. As the standard deviation from the mean is rather small, this suggests that selecting a section, within a beam of length L, that contains a photon, approaches 100%. We also classified different sub-Poissonian light sources and found that the quantum dot was a natural fit in the second class of sub-Poissonian light, and as such could be used as a source.

Having established that the quantum dot was a natural fit for this type of questioning, our next order of business was to establish the exact mechanism behind the quantum dot. We characterized the core-shell quantum dot as being a semi-conductor surrounded by a secondary substance which adds a confining potential. This potential creates a spectrum of bound states, and in the case of the quantum dot, we have three, rather than two states, to consider. With this understanding, the next step was to understand the exact mechanism that allowed the quantum dot to operate - The biexciton-exciton cascade. Finally the details necessary for our experimentation from the Reimer group's quantum dot were compiled for future reference.

Finally, we needed a framework to take this collective information and implement it to get a model. The Lindblad master equation was used, which is a generalized extension of the Hamiltonian formalism. In this framework, the system, the environment, as well as the coupling between the two are characterized by separate Hilbert spaces, but can be tensored to form a single Hilbert space. For the purposes of this thesis, we chose to use basis vectors of the quantum dot state to characterize our Hamiltonian. However, this is done with the careful understanding that each Hilbert space was unique and separate. Finally, the collapse operators that detail how the system interacts with the environment are considered resulting in equation (2.4.4).

The above considerations are utilized in the development of the model for quantum dot Rabi oscillations. However, we run into three challenges that give us some difficulty. The first is that we are dealing with a three-level system, rather than just two. Despite this, we are able to create basis vectors in three dimensions to represent our states. Secondly, the Hamiltonian written in (Huber, et al., 2016) is not conducive to QuTiP. As such, transformation given in (Bajcsy, 2022), was considered and a new

set of operators are defined that are implementable under QuTiP. Finally the Gaussian short pulse used from (Fischer, Dynamical Modeling of Pulse Two-Photon Interference, 2016) did not lend to observing Rabi oscillations. Therefore in order to make it work, we changed the standard deviation t_p to be within the same order of magnitude as the amplitude, Ω, of the Gaussian pulse. With these considerations, we ended up with a model that represented the Rabi oscillations for ground, exciton, and biexciton populations.

This model was successful in its representation of these groups as the behaviours demonstrated in the graphs made sense with respect to the behaviour expected from a quantum dot. For example, damping prevented the biexciton population from reaching a max 100% occupation at t_0. The graphs also demonstrated damping by the peaks diminishing in height, all three oscillating about the 35% probability for occupation. While this is a successful start, there are other considerations that must be made before this can be considered a conclusive model.

- QuTiP uses natural units and as such implementing a model that takes in the parameters of the Reimer group's quantum dot proved to be difficult
- Without implementing values that are reasonable to a quantum dot, it is difficult to compare it to the model provided in equation 2.1.18.

If the model is changed to account for these considerations, we can then confirm whether or not it confirms the quantum nature of the quantum dot. However, given that multiple sources and readings can be used to visually corroborate the results; I believe that we are certainly on the right track.

Acknowledgements

I would like to thank everyone who advised, guided, and provided me with the resources to develop and write this thesis. I would first like to thank Dr. Michael Reimer, for his kind and knowledgeable supervision and guidance. I came into this program not knowing how to handle a research question, and now I feel more confident in my problem-solving abilities. I would like to thank the members of the Quantum Photonics Devices group for allowing me to attend their group meetings and even contribute by presenting results from research papers. Your informative discussion helped me develop a better understanding of the field. In particular, I'd like to thank Sonell Malik and Matteo Pennacchietti for their tireless help and in helping find relevant resources for my thesis.

I'd also like to thank my family and friends for their unyielding support, I could not have completed this research without you. In particular, my loving husband, who has repeatedly picked me up when I felt as though I was not good enough. My parents, Jayaratnam and Chandrika, for their warm support of my pursuit of knowledge. To Kai who relentlessly tutored me throughout my undergraduate career, whose knowledge I greatly benefitted from. And finally Meagan and Nicole, I would not be anywhere near where I am without you.

Finally, I would like to acknowledge that I completed my research on the promised territory of the Haudenosaunee, Anishinaabe, and Attawandaron peoples. The University of Waterloo is situated on the Haldimand Tract, the land promised to the Six Nations that includes ten kilometers on either side of the Grand River.

Bibliography

Ahmadi, A. (2019). *Towards On-demand Generation of Entangled Photons with Quantum Dots.* Waterloo.

Bajcsy, M. (2022, October 6). ECE 770. *Lecture #9*. Waterloo, Ontario, Canada.

Davidovich, L. (1996). Sub-Poissonian Processes in Quantum Optics. *Reviews of Modern Physics*, 127-173.

Feranchuk, I., & Leonov, A. (2008). Analytical analysis of the “collapse-revival” effect in the Jaynes–Cummings model. *Physics Letters A*, 517-520.

Fischer, K. A. (2016). Dynamical Modeling of Pulse Two-Photon Interference. *New Journal of Physics*.

Fischer, K. A., Hanschke, L., Kremser, M., Finley, J. J., Muller, K., & Vucokvic, J. (2017). Pulsed Rabi oscillations in quantum two-level systems:. *Quantum Science and Technology*.

Fox, M. (2006). *Quantum Optics.* Oxford University Press.

Huber, T., Osterman, L., Prilmüller, M., Solomon, G. S., Ritsch, H., Weihs, G., & Predojević, A. (2016). Coherence and degree of time-bin entanglement from quantum dots. *Physical Review B*.

Leica. (2017, November 15). *The Fundamentals and History of Fluorescence and Quantum Dots*. Retrieved from Leica-Microsystems: https://www.leica-microsystems.com/science-lab/the-fundamentals-and-history-of-fluorescence-and-quantum-dots/#:~:text=Quantum%20Dots%20(or%20%22Qdots%22,Petersburg

Manzano, D. (2020). *A Short Introduction to the Lindblad Master Equation.* Granada.

Matthias, B., Lenhard, A., Chunniall, C., & Becher, C. (2016). Highly efficient heralded single-photon source for telecom wavelengths based on a PPLN waveguide. *Optics Express*, 23992-24001.

Nexdot. (n.d.). *Quantum Dots History*. Retrieved December 2022, from nexdot: https://nexdot.fr/en/history-of-quantum-dots/

Papoyan, A., & Shmavonyan, S. (2021). Signature of optical Rabi oscillations in transmission signal of atomic vapor under continuous-wave laser excitation. *Optics Communications*.

PR Newswire. (2019, February 23). *Benzinga*. Retrieved from The History and Future of Quantum Dots: https://www.benzinga.com/pressreleases/19/02/r13231898/the-history-and-future-of-quantum-dots

reductionista. (2016, October 20). *Spin Representation in 3D*. Retrieved from Physics Stackexchange: https://physics.stackexchange.com/questions/287542/spin-representation-in-3d

Sigma Aldrich. (n.d.). *Quantum Dots*. Retrieved from Millipore Sigma: https://www.sigmaaldrich.com/CA/en/technical-documents/technical-article/materials-science-and-engineering/biosensors-and-imaging/quantum-dots

Stievater, T., Li, X., & Steel, D. (2001). Rabi Oscillations of Excitons in Single Quantum Dots. *Physical Review Letters*.